

Cell Reports, Volume 36

Supplemental information

**One-shot identification of SARS-CoV-2 S RBD
escape mutants using yeast screening**

Irene M. Francino-Urdaniz, Paul J. Steiner, Monica B. Kirby, Fangzhu Zhao, Cyrus M. Haas, Shawn Barman, Emily R. Rhodes, Alison C. Leonard, Linghang Peng, Kayla G. Sprenger, Joseph G. Jardine, and Timothy A. Whitehead

This PDF file includes:

Figures S1 to S5

FIGURES

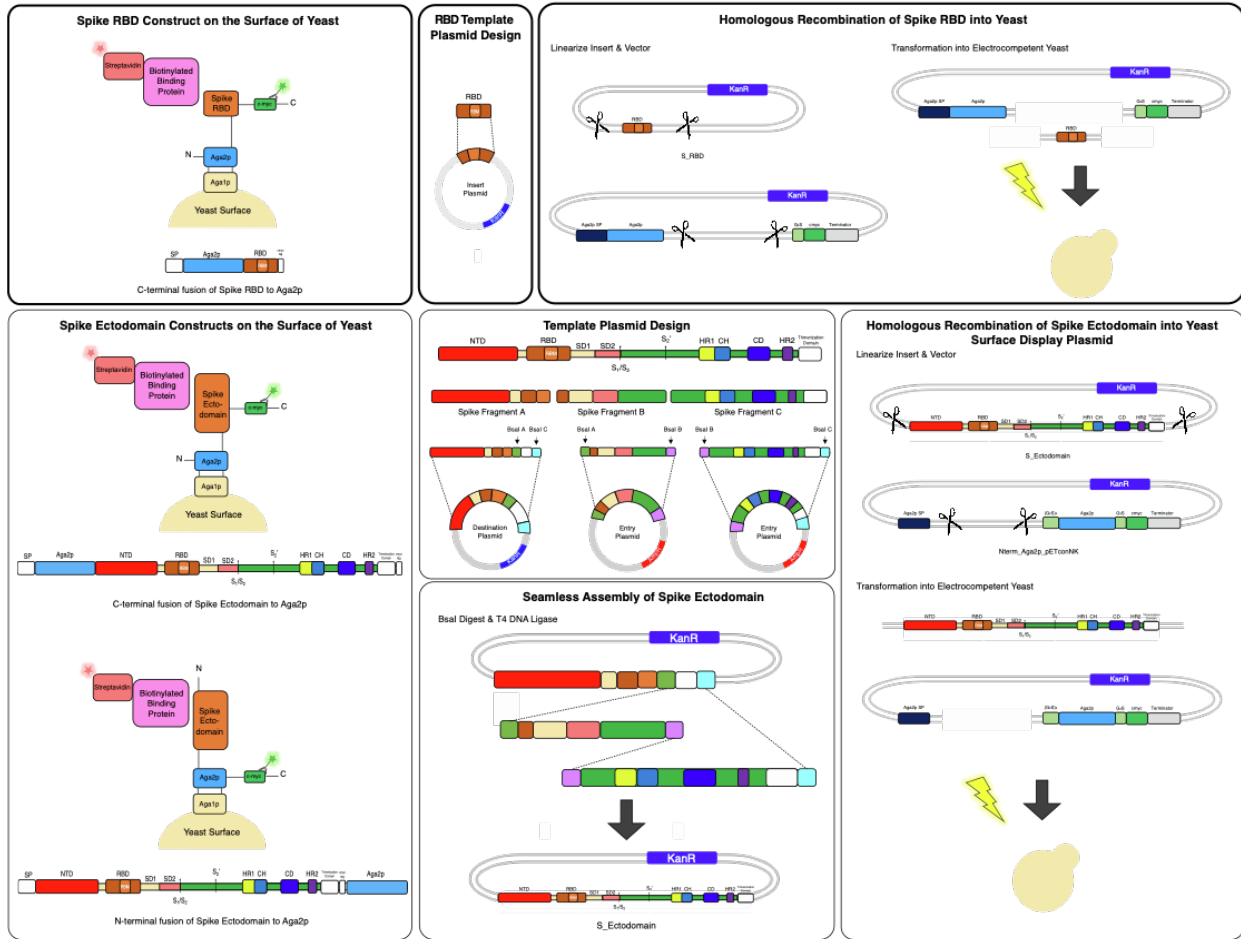


Fig. S1. Overview of yeast display constructs used in screening S RBD and prefusion stabilized S ectodomain libraries. Related to STAR Methods.

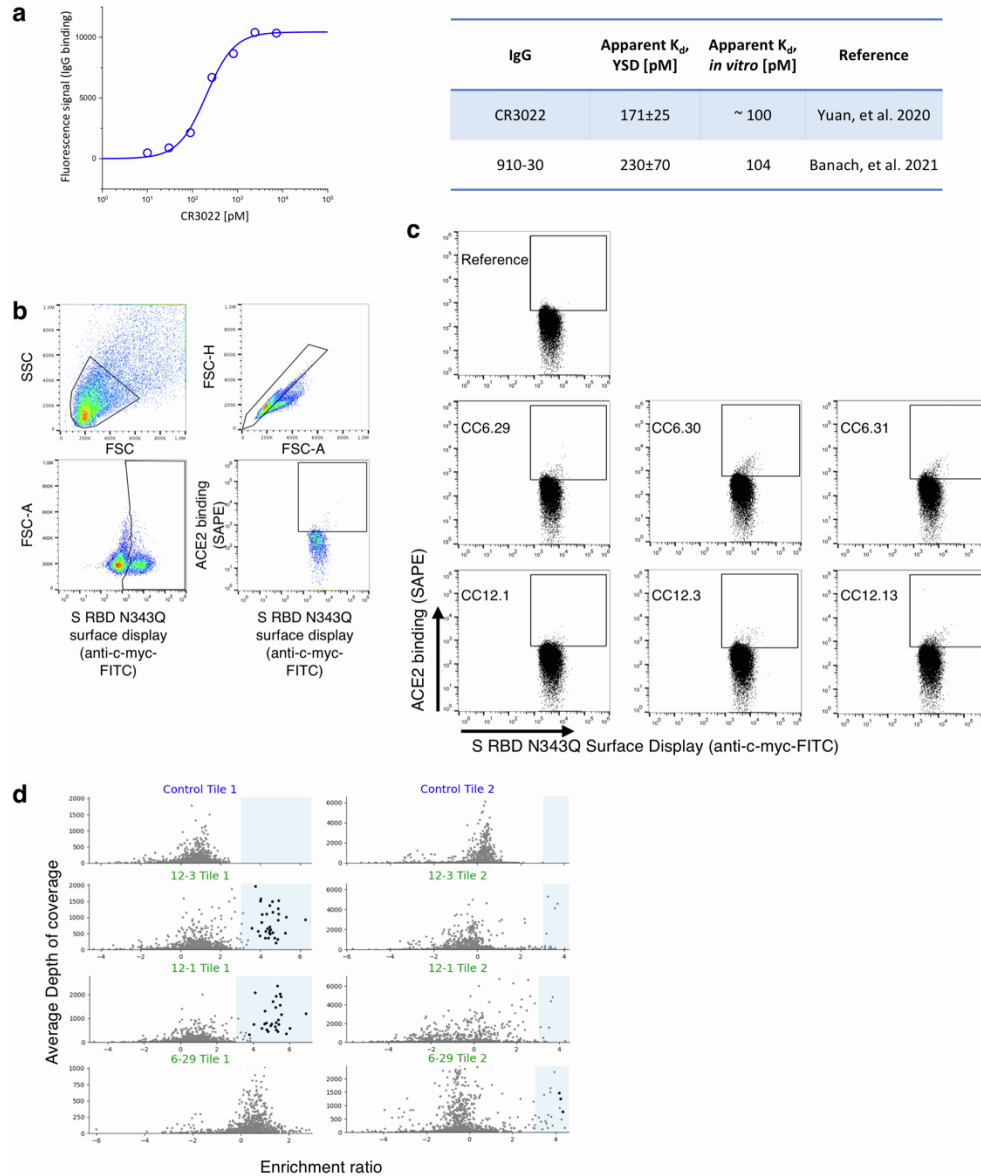


Fig. S2. Development and screening of yeast libraries of S RBD. (a.) Yeast cell surface titrations of non neutralizing CR3022 IgG against aglycosylated S RBD yield an apparent K_D of 171 ± 25 pM. Technical triplicates were performed ($n = 3$), and error reported is 2 s.e.m. Data for the HKU 910-30 nAb is from Banach et al, 2021. (Yuan, Wu, *et al.*, 2020; Banach *et al.*, 2021). (b.) Representative sorting gates used for all S RBD escape mutant FACS screens. The four gates were SSC/FSC; FSC-H/FSC-A to discriminate single yeast cells; FSC-A/FITC+ to select cells displaying the RBD on their surface; and SAPE⁺/FITC⁺ to identify mutants that allow ACE2 binding in the presence of $10 \mu\text{g}/\text{mL}$ antibody. Shown here are gates for the antibody CC6.29. (c.) Sorting gates for competitive binding experiments. PE/FITC cytograms for aglycosylated S RBD yeast libraries sorted using competitive binding with ACE2-Fc. The top cytogram shows the control experiment with no ACE2 labeling. Gates represent the top 2% of the FITC⁺ cells by PE signal for each antibody used in the study. (d.) Per-mutation enrichment ratio (ER) distributions as a function of average depth of coverage. control (top) and CC12.3, CC12.1, CC6.29 nAb competing experiment (bottom). ER thresholds determined for FDR = 1 are shown in the control

panels (top). Hits (with ER greater than the threshold at $p \leq 0.01$) are shown with larger black dots. Related to Figure 1.

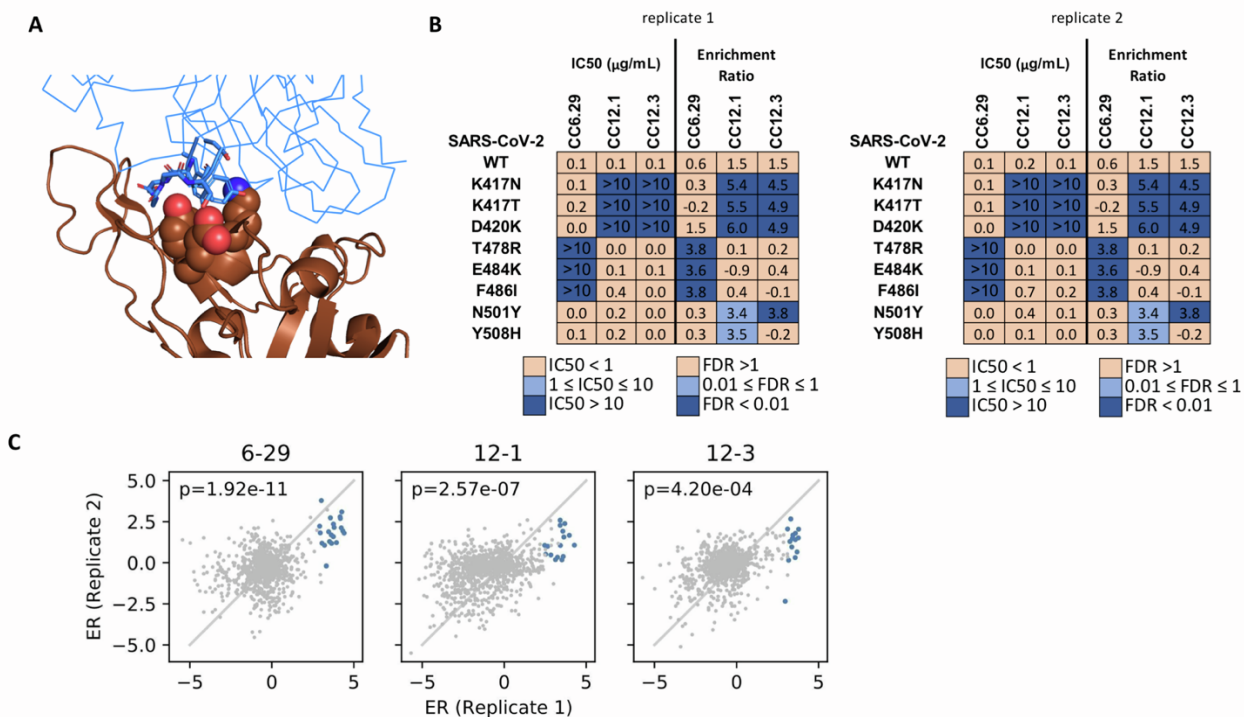


Fig. S3. Replicates and structural validation of escape mutant hits. (a.) Structural recognition of S RBD (chocolate cartoon) by nAB CC12.1 (PDB ID 6XC2, blue ribbon). S positions K417, D420, Y421 are shown as spheres and the CDR H2 and key CC12.1 residues are shown as sticks. **(b.)** MLV-based SARS-CoV-2 pseudo-virus neutralization assays for SARS-CoV-2 RBD variants. Data shown are replicates of the neutralization assays repeated on separate days (replicate 1 - day 1; replicate 2 - day 2). IC50 neutralization values shown are averages of two technical replicates. Replicate 1 data is also presented in Figure 1j of the main text. **(c.)** Comparison between biological replicates for S RBD positions 437-527 for CC6.29, CC12.1, and CC12.3. Escape mutant hits identified in replicate 1 are shown as closed blue circles (a $p \leq 0.01$ for an FDR < 1). p-values are calculated using a one-sided Welch's t-test with the alternative hypothesis that the mean enrichment ratio from the replicate 2 hits are > the mean enrichment ratio from the replicate 2 non-hits. Related to Figure 2.

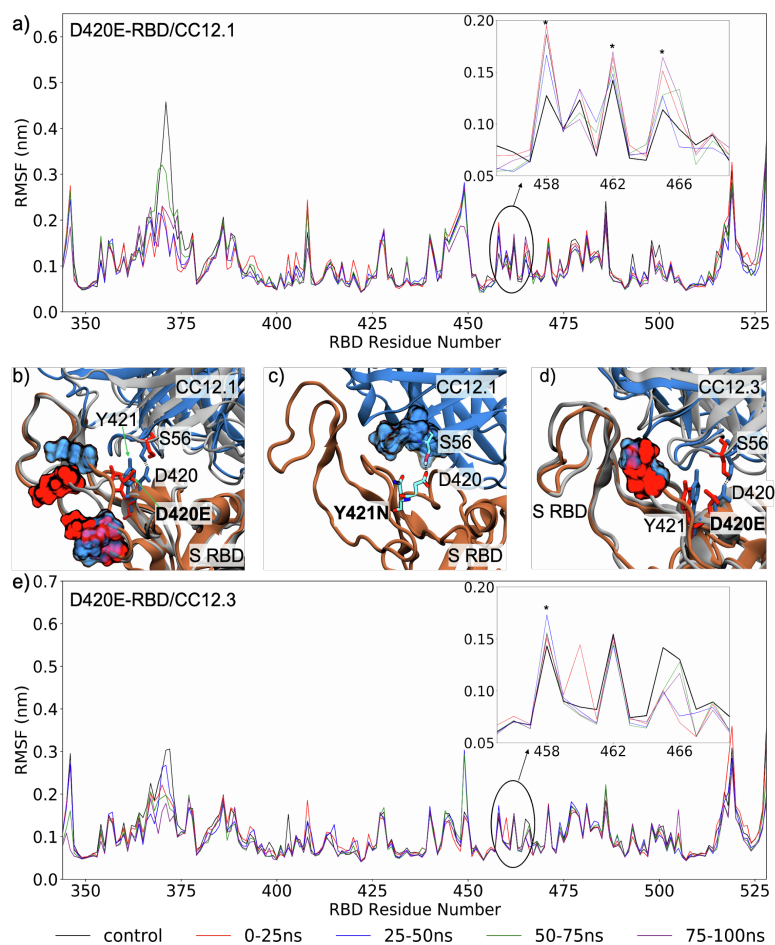


Fig. S4. (a) Comparison of the root mean square fluctuation (RMSF) profile of CC12.1 in complex with wildtype/control S RBD (averaged across the 100 ns production run) and S RBD with the D420E mutation (averaged across 25 ns intervals). (b) Structural mapping of highly fluctuating residues on S RBD with the D420E mutation, identified in panel (a), when complexed with CC12.1. Wildtype and mutant RBDs are shown in brown and gray and CC12.1 in blue and gray, respectively, while residues are colored blue for wildtype RBD and red for the mutant RBD; highly fluctuating residues are shown in surface representation. (c) MD snapshot showing the proposed mechanism of escape of S RBD from CC12.1 through mutation Y421N. (d) Structural mapping of highly fluctuating residues on S RBD with the D420E mutation, identified in panel (e), when complexed with CC12.3. (e) Comparison of the RMSF profile of CC12.3 in complex with wildtype S RBD and S RBD with the D420E mutation. Related to Figure 4.

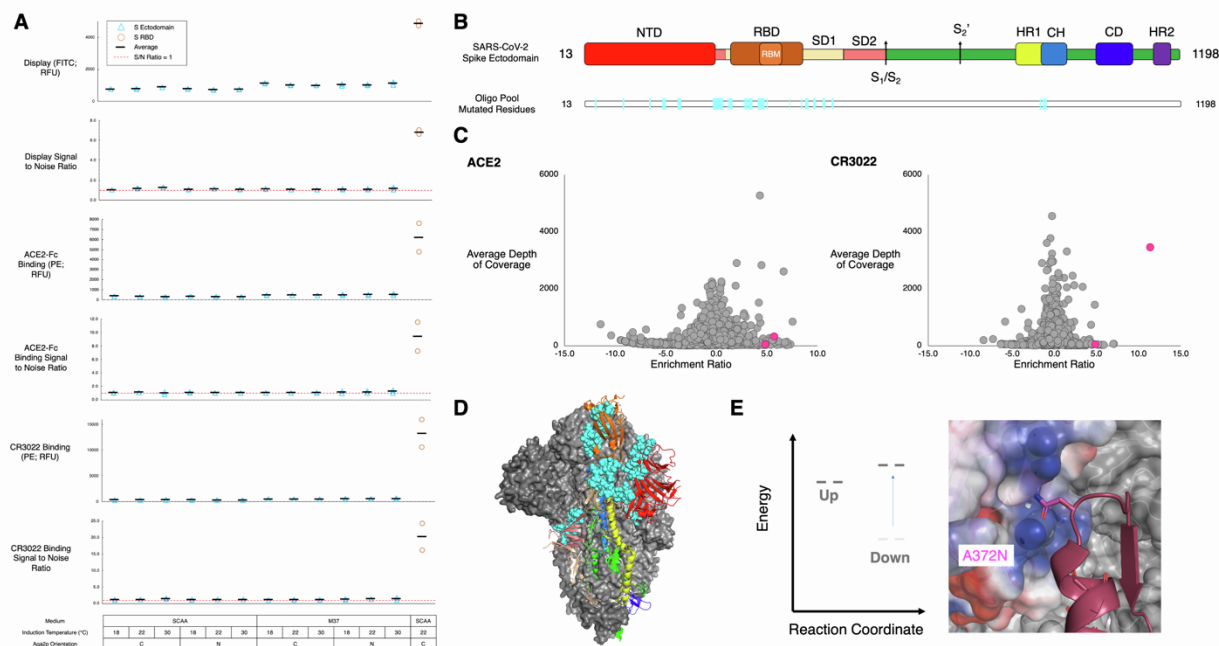


Fig. S5: Yeast surface display screening and putative hits for SARS-CoV-2 prefusion stabilized S ectodomain. (A) FITC signal (RFU), FITC signal to noise ratio, and PE signal (RFU) and PE signal to noise ratio for both ACE2-Fc and CR3022 are shown for biological replicates of spike ectodomain with differing media, induction temperatures, and orientation of Spike relative to Aga2p (blue triangles). The FITC fluorescence derives from an anti-cmyc FITC antibody that recognizes a C-terminal cmyc epitope tag for displayed protein, while the PE signal is from biotinylated ACE2-Fc or CR3022 subsequently labeled with streptavidin-PE. The concentration of the secondary binding protein for the S ectodomain was 500nM ACE2-Fc and 500nM CR3022. FITC signal (RFU), FITC signal to noise ratio, and PE signal (RFU) and PE signal to noise ratio for both ACE2-Fc and CR3022 shown for S RBD at optimal conditions (orange circles). The concentration of secondary binding protein for the S RBD is at 1 nM, which is at saturation. (B) Spike ectodomain schematic with labeled and colored boundaries. Below schematic is the locations of the mutated residues in the oligo pool, cyan, as well as locations of the top identified hits shown in magenta. NTD: N-terminal domain, RBD: receptor-binding domain, RBM: receptor-binding motif, SD1: subdomain 1, SD2: subdomain 2, S₁/S₂: furin cleavage site, S₂' : S₂' cleavage site, HR1: heptad repeat 1, CH: central helix, CD: connector domain, HR2: heptad repeat 2. (C) Average depth of coverage vs. Enrichment ratio for single mutants for (left) ACE2 and (right) CR3022. All mutations are shown in gray with the two hits (K113I & A372N) colored magenta. (D) Prefusion spike trimer shown with domains colored as they are in panel B. RBD is shown in the up conformation and along with SD1 and SD2 is shown on the same spike monomer. The NTD and S2 subunits are shown on a neighboring monomer. Oligo pool mutated residues are represented as cyan spheres. (E) Putative reaction coordinate and interaction of hit A372N in the spike ectodomain. A372N is hypothesized to destabilize the down protomer by steric repulsion with an adjacent 'down' protomer. Related to Figure 4.